20

High Power Tunable Tm^{3+}-fiber Lasers and Its Application in Pumping Cr^{2+}:ZnSe Lasers

Yulong Tang and Jianqiu Xu
Shanghai Institute of Optics and Fine Mechanics
Chinese Academy of Science, Shanghai 201800,
China

1. Introduction

1.1 Research background

Interest in the Tm^{3+}-doped fiber laser originates from its emission band in the range of 1400-2700nm lying between the bands of Er^{3+} and Nd^{3+} ions. Since the advent of double-cladding configuration of fiber and the recent technological development of high-power laser diodes, output power (performance) of Tm^{3+}-doped fiber lasers has scaled exponentially. Up to date, the maximum output achieved in Tm^{3+}-doped fiber lasers has been comparable with that from Yb^{3+}-doped fiber lasers. Laser beam in the 2~3μm wavelength range has wide applications. First, it is a good candidate in laser microsurgery due to high absorption of water in this spectral region thus can provide high-quality laser tissue cutting and welding. In addition, this wavelength-range laser has potential applications in environment monitoring, LIDAR, optical-parametric-oscillation (OPO) pump sources, and so on [1-4].

For obtaining laser emission in the mid-infrared wavelength region, the Tm^{3+}-doped fiber is an excellent candidate due to several unique advantages it possesses. First, the Tm^{3+}-doped fiber has a strong absorption spectrum that has good overlap with the emission band of commercially available AlGaAs laser diodes, which have been significantly developed and are being developed with an unprecedented speed. Second, the specific energy-level structure of Tm^{3+} ions provides the Tm^{3+}-doped fiber laser a special advantageous energy-transfer process-the $^3H_4+^3H_6 \rightarrow ^3F_4+^3F_4$ cross relaxation process. In this process, two excited-state ions can be obtained with depletion of just one absorbed pump photon. With an appropriately high doping level, the cross relaxation process can offer a quantum efficiency close to two, which greatly improves the efficiency of the Tm^{3+}-doped fiber laser. Thirdly, the Tm^{3+}-doped fiber has a very broad emission band, spanning over more than 400 nm. This feature offers the Tm^{3+}-doped fiber laser an especially high-degree wavelength tunability, which is very useful in applications such as spectroscopy, atmospheric sensing and so on.

1.2 Host material of Tm^{3+}-doped fiber

For laser ions, the combination of the energy gaps between the excited level and the one just below it and the maximum phonon energy (MPE) plays an important role in the nonradiative relaxation rate, which in turn has a significant influence on the laser efficiency originated from the excited states. For Tm^{3+} ions, different host materials show a great

Source: Frontiers in Guided Wave Optics and Optoelectronics, Book edited by: Bishnu Pal,
ISBN 978-953-7619-82-4, pp. 674, February 2010, INTECH, Croatia, downloaded from SCIYO.COM

difference in the MPE value. Two most common host materials used for Tm^{3+} fibers are silica and fluoride glass. Their MPE differs about several times, being 1100 cm^{-1} (silicate) and 550 cm^{-1} (fluorides), respectively [5]. Large MPE of the silicate glass fiber limits its infrared transparency range less than 2.2 μm and improves its multiphonon relaxation rates. Therefore, fluoride fibers are preferred as the host material for Tm^{3+} ions to achieve comparatively longer-wavelength emission.

In Tm^{3+}-doped fiber lasers, the $^3F_4 \rightarrow {}^3H_6$ transition is usually exploited to achieve the ~2 μm high-power laser output. This transition can produce a very wide emission band, providing a broad tuning range for lasers and a wide optical bandwidth for amplifiers. However, the relaxation of the $^3F_4$ level is predominantly nonradiative. The measured lifetime of the $^3F_4$ level for Tm^{3+} doped silica fiber is just 0.2 ms [6] showing a high nonradiative rate thus low quantum efficiency. Therefore, Tm^{3+}-doped fiber lasers usually have high laser thresholds. On the contrary, Tm^{3+}-doped fluoride fiber lasers have comparatively lower thresholds due to a low MPE. The high nonradiative rate, however, does not impair laser slope efficiency, because stimulated emission will dominate nonradiative relaxation once the laser has been risen above threshold. Due to high damage threshold and the very effective modified chemical vapor deposition (MCVD) technique for fiber fabrication, Tm^{3+} silica fibers are usually chosen to construct high-power 2-μm fiber lasers.

1.3 Fiber design for cladding pumping

Tm^{3+}-doped fibers can be either core pumped or cladding pumped. In the past, the fiber laser was usually core pumped. The fiber core areas are generally <100 $μm^2$, which limit the power scalability because this method depend on expensive high-beam-quality pump sources. Since the invention of double cladding fiber configuration with a larger cladding area >10000 $μm^2$, together with a high numerical aperture (NA) of 0.3-0.55, output power of Tm^{3+}-doped fiber lasers can be greatly improved by use of high-power diode-arrays as pumping sources.

In the design of fibers for cladding pumping, the core of the fiber is usually made small (such as less than 5 microns) to guide a single-transverse mode (LP_{01}). The cladding generally has a much larger cross section (several-hundred-micron diameter) for high-power launching, and the shape of the cladding can be flexible with novel consideration. The shape of the inner cladding of the fiber has a great impact on the absorption efficiency of launched pump light. In the past, the inner cladding is used to be circularly symmetric, which can be drawn with ease and is compatible with the pig-tail fiber of the pump LD. However, the circular symmetry will make large portion of the pump light to be skew light, greatly reducing the absorption efficiency of doping ions. In order to improve the utility efficiency of pump sources, and take the pump light shape into account (compatible with the inner cladding shape), various double cladding fiber structures are invented, as shown in Fig. 1. By using these double cladding fibers, the pump efficiency is significantly enhanced.

1.4 Tm^{3+}-doped fiber laser cavity structure

The fiber laser resonator can be very simple when it is in free-running regime. The commonly adopted three kinds of fiber laser resonators, defined as Fabry-Perot resonator, are shown in Fig. 2. Fig 2 (a) is the simplest cavity, the pump light is launched into the fiber through a dichroic mirror, which is high reflective for laser light. Laser oscillation forms between this dichroic mirror and the distal-end fiber facet (~4% Fresnel reflection). In this cavity configuration, addition of output coupler or pump-light reflector will improve the

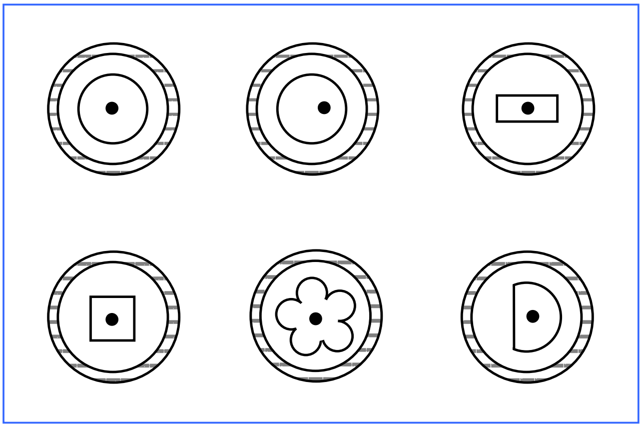

Fig. 1. Various shape of the double cladding fiber cross section

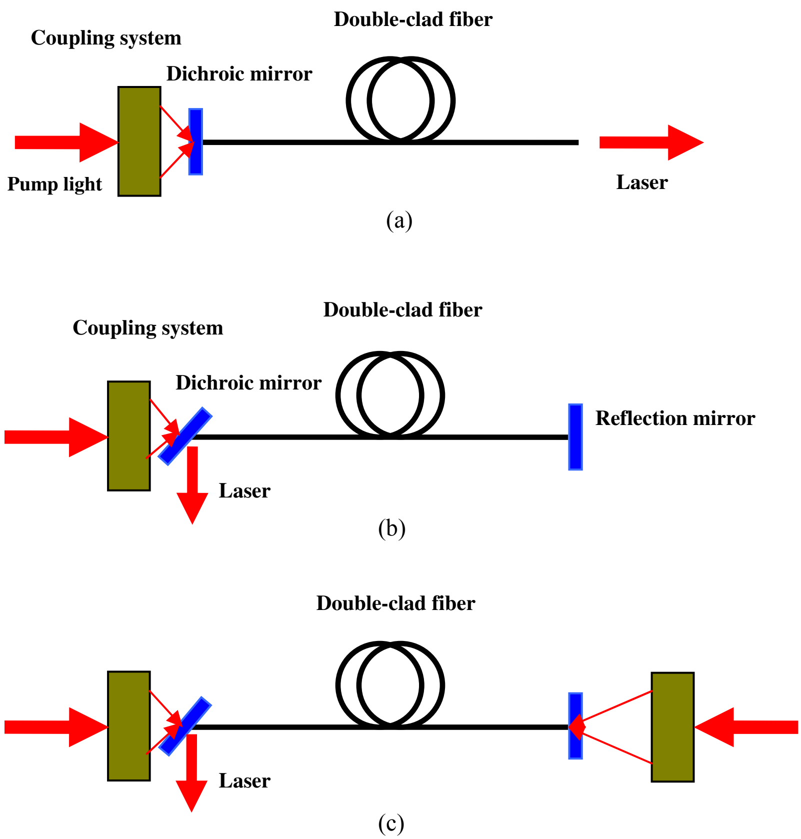

Fig. 2. Tm^{3+}-doped fiber laser resonators (a) Single-end forward pumping; (b) Single-end backward pumping; (c) Double-end pumping.

optical efficiency of the fiber laser. In Fig 2 (b), the pump light is launched into the fiber from the output end, and the dichroic mirror is set at 45 degree with respect to the fiber axis for extracting laser output. At the distal fiber end, a signal high reflection mirror is added to form the laser resonator. The cavity of Fig 2 (c) is used to further improve the pump power that can be launched into the fiber for the aim of power scaling.

In order to realize wavelength tuning, and at the same time obtain narrow-width laser spectrum, a bulk gratings can be put in the cavity as the output coupler. However, wavelength-tuning with bulk grating is inconvenient, and brings laser instability. The commonly used wavelength-tuning fiber laser resonator is constructed by using fiber Bragg gratings as the feedback device and output coupler, as shown in Fig. 3. This kind of fiber laser resonator can provide not only wavelength tuning, but also narrow spectral width and high stability.

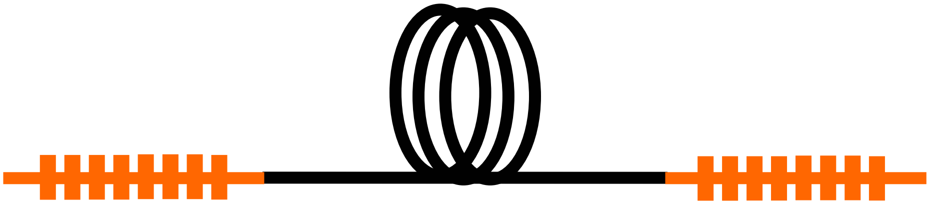

Fig. 3. Complete-fiber resonator with fiber Bragg grating.

1.5 Spectral characteristics of Tm^{3+}-doped silica fiber

Our aim is to focus on the development of high-power ~2μm fiber laser, so the description about the spectral characteristics is only confined to the Tm^{3+}-doped silica fiber. The absorption spectrum of Tm^{3+}-doped silica fiber is shown in Fig. 4 [7]. This spectrum has strong absorption near 790 nm, which has good overlap with the emission band of present fully developed AlGaAs diode lasers. This feature of the Tm^{3+}-doped fiber laser makes the pump process comparatively easier and less expensive, offering an exciting potential for power scaling in the 2-μm wavelength range.

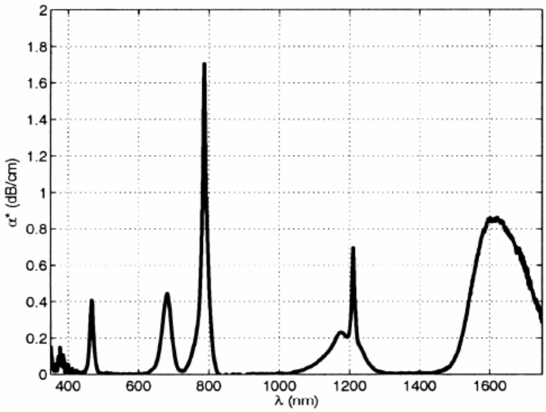

Fig. 4. Absorption spectrum of Tm^{3+}-doped silica fiber

The simplified energy-level diagram of Tm^{3+} ions is shown in Fig. 5. The pump light at ~790 nm excites Tm^{3+} ions from $^3H_6$ to $^3H_4$, which then nonradiatively decay to the upper laser level of $^3F_4$ with a fluorescence lifetime of 0.55 ms [8]. The transition from $^3F_4 \rightarrow {^3H_6}$ will radiates photons at wavelength of ~2μm. Due to large Stark splitting of the lower laser level (the ground state level), the Tm^{3+}-doped fiber laser is a quasi-four-level system.

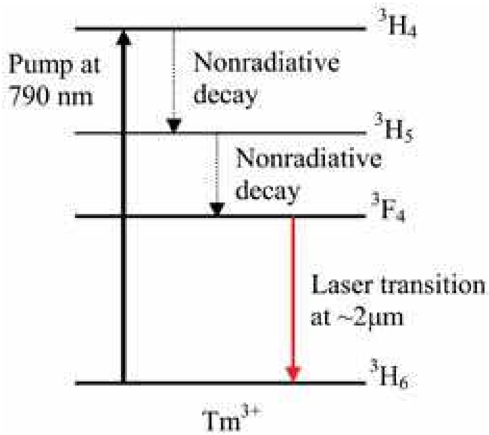

Fig. 5. The simplified energy-level diagram of Tm^{3+} ions

The special energy-level structure of Tm^{3+} ions provides the Tm^{3+}-doped silica fiber laser the advantageous **cross relaxation** process ($^3H_4+{^3H_6}\rightarrow{^3F_4}+{^3F_4}$). With this process, high quantum efficiencies can be achieved in Tm^{3+}-doped fiber lasers by appropriately improving the ion doping concentration. The cross relaxation process, as shown in Fig 6, can produce >100% quantum efficiencies for Tm^{3+}-doped fiber lasers [9-10]. In experiment, slope efficiency larger than 60% has been achieved (quantum efficiency>150%) in Tm^{3+}-doped fiber lasers [11-12].

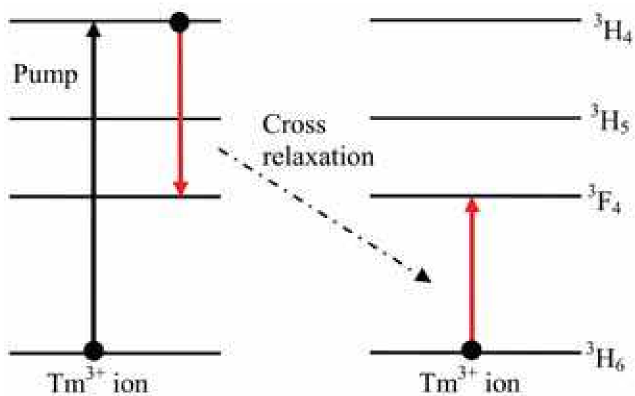

Fig. 6. Cross relaxation between Tm^{3+} ions.

In Tm^{3+}-doped silica fiber lasers, high-degree Stark splitting of the $^3H_6$ level by local electric field produces a broad emission band (>400 nm), as shown in Fig. 7 [13]. This special broad emission band makes Tm^{3+}-doped fibers very suitable for wavelength tuning.

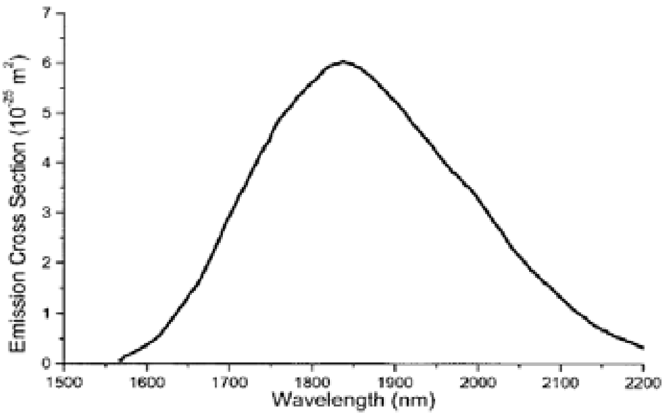

Fig. 7. The emission spectrum of the $^3F_4 \rightarrow ^3H_6$ transition in Tm^{3+}-doped silica fiber

1.6 Pump sources

With the fully development and decreasing cost of AlGaAs diode lasers, diode lasers are the primary and ultra most preferred pump source in pumping ~2μm Tm^{3+}-doped fiber lasers at present. The 790-nm diode lasers pump Tm^{3+} ions to the $^3H_4$ level, which can lead to the advantageous cross relaxation process, greatly enhancing the quantum efficiency of Tm^{3+}-doped fiber lasers. From the absorption band of Tm^{3+} ions, light sources at other wavelength can also be used as the pump. As shown in Fig. 8, apart from 790nm, the pump sources include the 1.064μm and 1.319μm output from Nd:YAG lasers, 1.09 μm from Yb-doped fiber lasers, and 1.57μm Er^{3+}-doped fiber lasers.

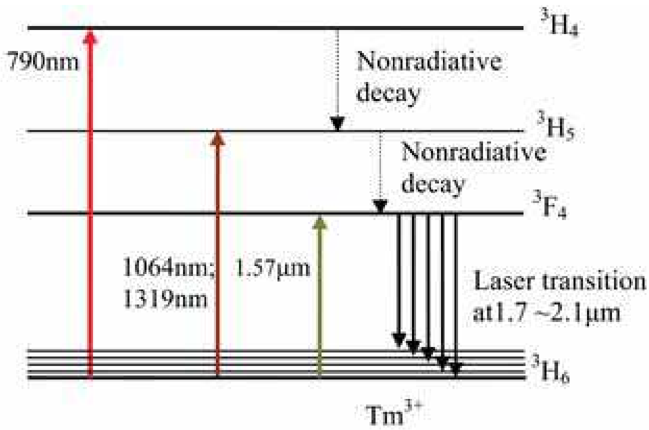

Fig. 8. The schematic of Tm^{3+} silica fiber with different pump wavelength.

The advantage of the 1.064 μm and 1.09 μm pumping is that Nd:YAG lasers and Yb-doped fiber lasers have been fully developed, which can be obtained with ease and low cost. This wavelength is used for the $^3H_5$-band pumping. Due to strong ESA, this band pumping leads to slope efficiencies less than 30% [14-15].

When the 1.319μm Nd:YAG laser is used as the pump source for Tm^{3+}-doped fiber lasers, the Tm^{3+} ions are pumped to the $^3H_5$ level. The small absorption cross section of the pump light limits the slope efficiency of the 1.319μm-pumped Tm^{3+}-doped fiber laser. Besides, at this wavelength, excited-state absorption of the pump is strong. Therefore, the slope efficiency of Tm^{3+}-doped fiber lasers with this kind of pump source is less than 25% [16].

When the Tm^{3+}-doped fiber laser is pumped at 1.57μm wavelength, the system is defined as a resonant pump structure due to the pump level ($^3F_4$) is also the upper laser level. Such a pump scheme has a small Stokes shift, thus can provide high operation efficiencies for Tm^{3+}-doped fiber lasers. With this pump technique, M. Meleshkevich reported a slope efficiency of 60% with respect to absorbed pump power [17]. However, this pump scheme cannot make use of the advantageous "cross relaxation" as the 790-nm pumping. Therefore, the highest efficiency is also less than that has been achieved in 790-nm-pumped Tm^{3+}-doped fiber lasers.

1.7 Recent power scaling of CW Tm^{3+}-doped fiber laser

The first ~2μm laser output from the $^3F_4 \rightarrow {}^3H_6$ transition in Tm^{3+}-doped silica fiber laser was achieved by Hanna et al in 1988 with a 797-nm dye laser as the pump source [18]. With the advent of AlGaAs diode lasers, diode-pumped Tm^{3+}-doped silica [19] and fluoride [20] fiber lasers were both realized in 1990.

The first high-power double-clad Tm^{3+}-doped silica fiber laser was reported by Jackson in 1998. The maximum output power is 5.4 W, and the slope efficiency is 31% [21]. In 2000, the output power was improved to 14 W with a slope efficiency of 46% [22]. In 2002, the 793-nm laser diode pumped Tm^{3+}-doped fiber laser has achieved a power output of 85 W with the slope efficiency of 56%. At the same power level, 75 W 2μm laser output was realized in an Yb-Tm codoped fiber laser, where ytterbium ions are used as sensitizing ions to facilitate pumping with 976 nm diodes. The slope efficiency however is just 32% due to the lack of "cross relaxation" process compared with those directly 790-nm pumped Tm^{3+}-doped fiber lasers [24]. In 2007, G. Frith reported a Tm^{3+}-doped fiber laser with output power improved to 263 W and the slope efficiency of 59% [25]. In 2009, the 2 μm output power from the Tm^{3+}-doped fiber laser was significantly enhanced to 885 W with a slope efficiency of 49.2% [26]. In addition, single frequency output has also been over 600 watts [27]. Further improving the 2-μm laser output over 1-kilowatt level, comparable with Yb-doped fiber lasers, is just a matter of time.

2. Short-length Tm^{3+}-doped silica fiber lasers

2.1 Introduction

Compared with long fiber lasers, short fiber lasers have many unique advantages. First, short fiber lasers can provide narrow-linewidth laser emission due to large axial mode spacing. From the equation [28]

$$\Delta \nu = \frac{c}{2nL}, \tag{1}$$

the shorter the fiber length, the larger the axial mode spacing. In a same broad gain spectrum, short fiber length leads to fewer axial modes obtaining enough gain to overcome cavity loss achieving oscillation. Therefore, the laser spectrum will be much narrower with shorter fiber length. Second, in pulsed laser operation, short fiber lasers are preferable to produce short pulse-width emission with high peak power. The laser pulse width can be expressed by [29]

$$\tau_p = \frac{r\eta(r)}{r-1-\ln r} \times \frac{2L}{c\delta_0} \, . \tag{2}$$

where, δ_0 is the single-pass cavity loss, η(r) is the energy extraction efficiency, r is the pump strength, L is the cavity optical length. We can see that the laser pulse width is proportional to the fiber length. Therefore, short fiber laser is preferred to achieved short pulse duration, thus achieve high peak power. In addition, short fiber lasers are free from the undesired nonlinear effects such as stimulated Raman, Brillouin scattering and so on.
Short-length Tm^{3+}-doped fiber lasers can be used to achieve single frequency output [7, 30-31], as well as moderate-level laser output [32] in the mid-infrared region. Such kind of compact mid-infrared laser device has great potentials in communication and integrated optical systems. Power scaling of short Tm^{3+}-doped fiber lasers will improve the utility of 2μm fiber lasers and speed the development of compact fiber laser systems.
In this section, short thulium-doped fiber lasers with high-power output are introduced. Besides, the performance dependence of such kind of laser on temperature and cavity parameters are discussed.

2.2 Experiment and CW output

The double-cladding thulium-doped fiber has a 30 μm diameter, 0.22 N.A. core doped with ~2wt.% Tm^{3+}. The pure-silica cladding, coated with a low-index polymer, has a ~410 μm diameter and a N.A. of 0.46. The cladding absorption coefficient at the pump wavelength (790 nm) is ~7dB/m. These fiber specifications of large fiber cross section, large ratio of core diameter to cladding diameter, high N. A. and high doping concentration make it possible to achieve high output power from short length of fibers. The pump source for the experiment is a single high-power LD bar, operating TM mode centered at 790 nm, shifting to ~793 nm at comparatively higher operating temperature. With this pump source, the maximum power launched into the fiber is near 12 W.
The laser cavity configuration is shown in Fig. 9 [33]. The laser pumping beam is reshaped first by a micro-prism stack, and then focused into a circular spot of ~0.5×0.5 mm diameter with a cylindrical lens and an aspheric lens. The focused pump beam is launched into the thulium-doped fiber through a dielectric mirror. The pump end of the fiber is butted directly to the dielectric mirror with high reflectivity (>99%) at 1850~2100 nm and high transmission (>97%) at 760~900 nm. The distal end of the fiber is directly butted to the output coupler with ~90% reflectivity at 1800~2000 nm to build a Fabry-Perot laser resonator. During the course of the experiments, the fiber is clipped between two copper sheets, which are closely fixed onto a water-cooling heat sink. The combination of a dielectric mirror (R>99%@1850~2100nm, T>99%@7 90 nm) and a Ge filter is used to extract the laser light and block the unabsorbed pump light.
Figure 10 shows the output power of a 7-cm length fiber laser as a function of launched pump power without water-cooling (40°C) [33]. When the cavity is constructed with an output coupler of 10% transmission, the laser has a threshold pump power of 135 mW and a maximum output power of 1.09 W. When the pump power is over 10 W, rollover of the output power occurred, which probably stemmed from large amount of heat generated in

the fiber due to large quantum defect. The slope efficiency of the fiber laser is about 9.6% with respect to launched pump power, which is much higher than that of silica based DFB fiber lasers [7, 32], but lower than that from a thulium-doped germinate glass fiber laser [31]. The comparatively low slope efficiency can be accounted by poor pump absorption due to relatively low doping concentration and short fiber length. Another alternative explanation can be related to the background loss of the silica-based fiber at wavelengths longer than 1.8 µm [34]. When the output coupler mirror is removed and only the 4% Fresnel reflection of the fiber end is used to complete the laser cavity, the maximum output power and slope efficiency decrease to 0.96 W and 8.7%, respectively. However, below 2.3 W of pump power, the fiber-end output coupler leads to slightly higher output power. Different output coupling seems to have little influence on the threshold pump power, which remains around 135 mW.

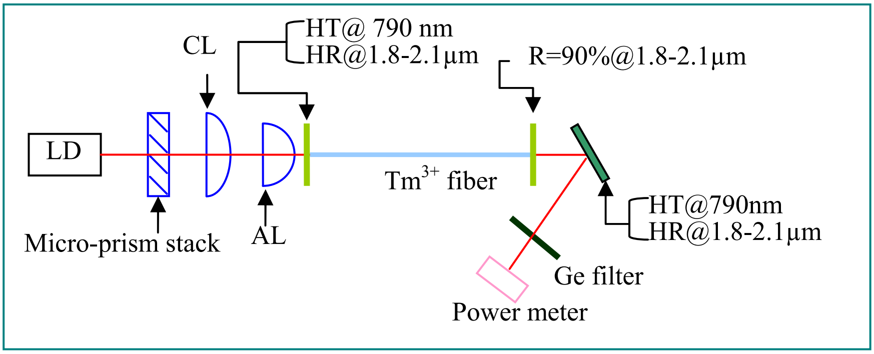

Fig. 9. Schematic diagram of the experimental setup. HT: high transmission; HR: high reflection; CL: cylindrical lens; AL: aspheric lens.

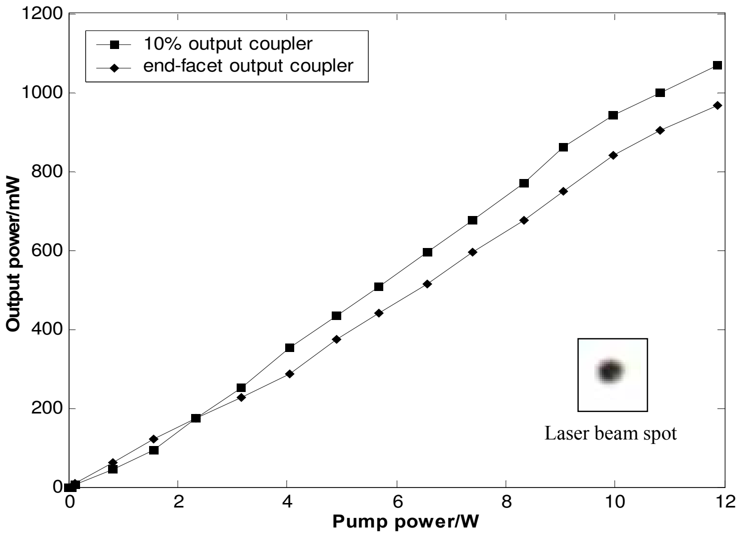

Fig. 10. Output characteristics of a 7 cm-length fiber laser with 10% output coupler and fiber-end-face coupler (R~4%). Inset is the laser beam spot.

In order to find out the influence of the spacing between the rear fiber end and the output coupler, a 6-cm-long fiber is used. The air spacing is denoted by L_s. This fiber laser is still operated with just air convectional cooling (40°C). The output characteristics are shown in Fig. 11 [33]. When L_s =0, a maximum output power of 496 mW and a slope efficiency of 4.6% can be obtained. When L_s =0.5 and 1 mm, the laser operation efficiency decreases greatly: the maximum output power reduces to 328 mW, and the slope efficiency decreases to 2.95%. This can be accounted by large reduction of the cavity Q factor by strong fiber-end diffraction loss. As far as L_s =0.5 mm and L_s =1 mm are compared, no significant different performance can be observed.

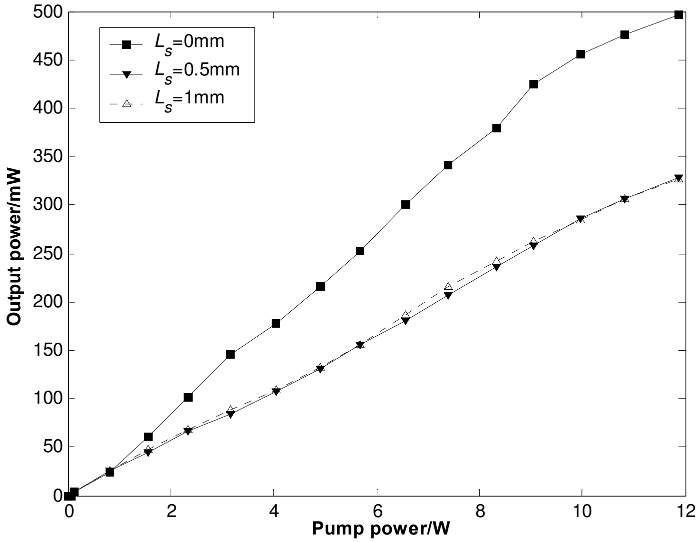

Fig. 11. Output characteristics of a 6 cm-length fiber laser with different air spacing between distal fiber end and output mirror.

2.3 Influence of temperature

In Tm^{3+}-doped fiber lasers, the ground-state level is Stark splitted into many sub levels. The Tm^{3+}-doped fiber laser is a quasi-four-level system, so the operation temperature has an important impact on the laser efficiency. For simplicity, we assume the ground state level of the Tm^{3+} ion is spited into just two sub levels N_1 and N_2. N_1 is the level where pump absorption starts from, and N_2 is the lower laser level. Between these two Stark levels, the population follows the Boltzman distribution [35]

$$\frac{N_2}{N_1} = e^{-\frac{E_2 - E_1}{kT}} , \tag{3}$$

where, E_1 and E_2 are energies of these two levels, k is the Boltzman constant and T is temperature. From the above expression, different temperatures will lead to different population distributions between N_1 and N_2, which in turn has an influence on the population inversion for the laser transition. Therefore, the laser operation temperature will have an important impact on laser efficiency.

A 5.5-cm long Tm^{3+}-doped fiber laser is constructed to observe the impact of the fiber operation temperature on the laser efficiency. The operation temperature of the fiber is controlled by changing the temperature of the circulating water through the copper heat-sink. Without water-cooling, the operation temperature of the fiber is around 40°C. With water-cooling, the operation temperature can be adjusted from ~0°C to 40°C. The output characteristic of the 5.5-cm-lenght fiber laser with different operation temperatures is plotted in Fig. 12 [33]. Both the maximum output power and slope efficiency exhibit a notable increase as the operation temperature of the fiber laser decreases from 40°C to 10°C. The maximum output grows from 345 mW to 531 mW, and the slope efficiency rises from 4% to 5.8%. The threshold pump power drops to 85 mW at operation temperature of 10°C. At high pump levels, a rollover of the output can be observed for all operation temperatures, which is accounted by saturation of pump absorption and distortion of the fiber end by high light intensity. At the maximum output level, the laser output fluctuation is less than 5% (as shown in the inset of Fig. 12), showing high stability of short-length Tm^{3+}-doped fiber lasers.

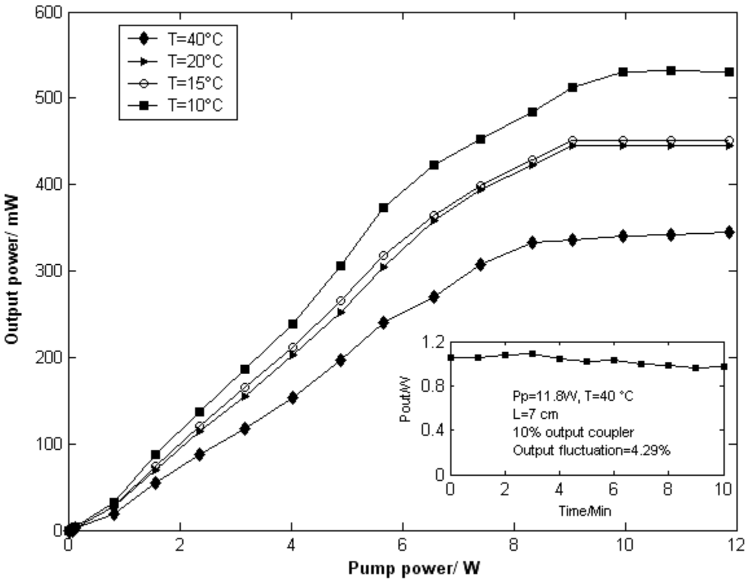

Fig. 12. Output characteristics of a 5.5 cm-length fiber laser with different operation temperatures; inset is the output power versus time (minute) at constant pump (11.8W) and operation temperature (40°C).

2.4 The laser spectra

Fig. 13 is the laser spectrum of the 5cm-length Tm^{3+}-doped fiber laser measured at pump power of 10 W (output of ~500mW). It is clear that the short fiber laser operates in few longitudinal modes. This is because that the fiber length is small, leading to a large longitudinal mode spacing, only few modes can obtain enough gain to initiate laser oscillation. The main spectral peak situates at 1970 nm, with a FWHM of ~3 nm. This spectral band width is much narrower than that obtained in the longer fiber laser [23], whose laser band width is tens of nm. Therefore, it is much easier to achieve single-frequency laser output with short-length Tm^{3+}-doped fibers. The existence of another small spectral peak indicates the mode competition in the short Tm^{3+}-doped fiber laser.

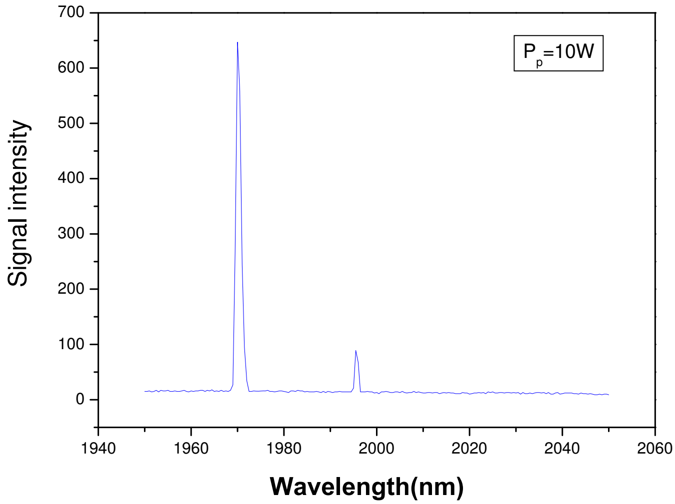

Fig. 13. Laser spectrum of the 5cm-length Tm^{3+}-doped fiber laser

The laser spectra of this short fiber laser under different pump power levels are shown in Fig. 14. When the pump power is 0.8 W, the laser only shows one spectral peak. The single-spectral-peak operation preserves with improvement of the pump to 2 W. When the pump is increased to 5W, laser operation changes from single spectral peak to two spectral peaks. At high pump level, mode hopping occurs, e.g. the main spectral peak changes to 1997 nm at the pump power of 8 W. The mode hopping phenomenon is probably due to changes of the cavity configuration parameters induced by the variation of the circumstance (such as fiber temperature or deformation of the cavity mirror).

3. High power ~2 μm Tm^{3+}-doped silica fiber laser and its wavelength tunability

The Tm^{3+}-doped fiber laser pumped by diode lasers has a great potential to scaling its output comparable to or even over the Yb^{3+}-doped fiber laser. This is because that Tm^{3+}-doped fiber can be pumped at around 790 nm, where efficient diode lasers are readily available. Another reason is that the Tm^{3+}-doped fiber laser can benefit from the cross-relaxation process, obtaining two excited Tm^{3+} ions for one pump photon. Therefore, the Tm^{3+}-doped fiber laser can provides, in theory, a maximum efficiency of 82% (a maximum

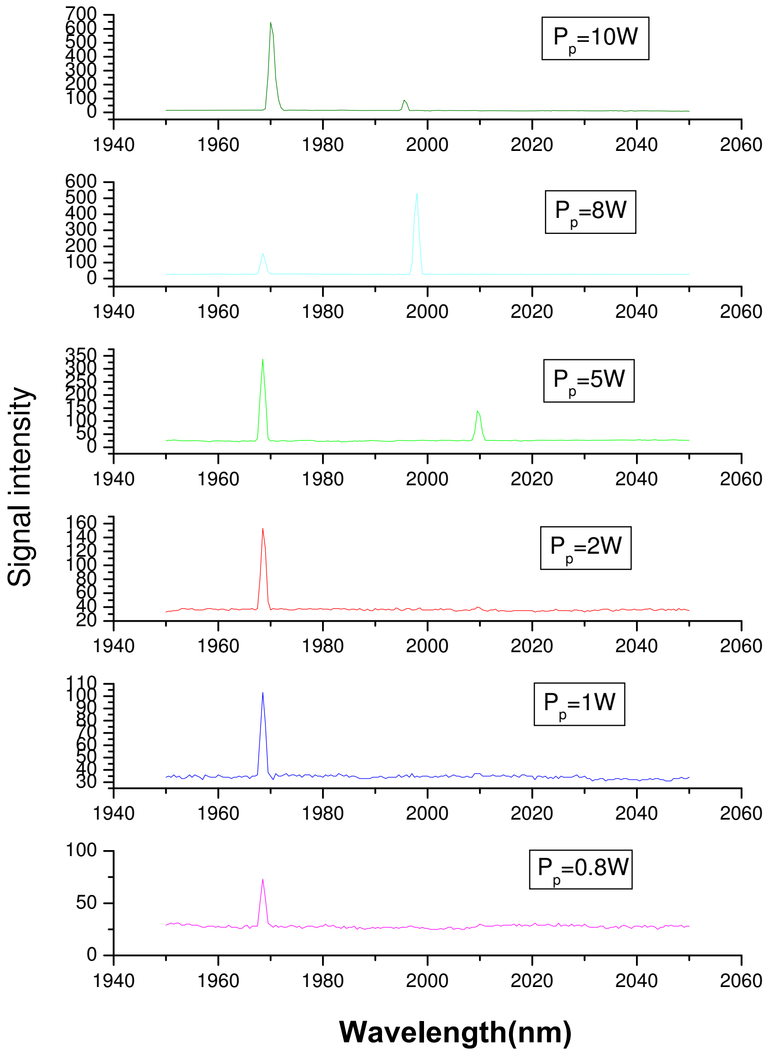

Fig. 14. Laser spectrum of the 5cm-length Tm^{3+}-doped fiber laser at different pump levels

quantum efficiency of 200%). Since 1998, the output power of double-clad Tm^{3+}-doped fiber laser has scaled steadily, especially when Al was codoped into the fiber to improve the Tm^{3+} doping level [36-37]. At present, the maximum CW output from the 2μm Tm^{3+}-doped fiber laser has arrived at 885W [26]. With further improvement of the pump diodes and pumping techniques, the 2μm output from the Tm^{3+}-doped fiber laser will be over 1 kilowatts and rise to tens of kilowatts.

3.1 Power scalability of Tm^{3+}-doped fiber laser

In this section, the power scalability and the limitation of Tm^{3+}-doped fiber lasers is analyzed and discussed. Detailed analysis shows that Tm^{3+}-doped fiber lasers have higher power scaling capabilities than that of Yb fiber lasers, i.e. higher power can be achievable from Tm^{3+}-doped fiber lasers than Yb fiber lasers. Thereafter, a 100-W CW Tm^{3+}-doped silica fiber laser with 60% slope efficiency is demonstrated experimentally and a design of twisted slab-like Tm^{3+}-doped fiber with the modal area of 5000μm^2 is proposed for high-power Tm^{3+}-doped fiber lasers.

3.1.1 Introduction

Compared with solid-state lasers, fiber laser has many advantages, such as good heat management (large surface to volume ratio), high beam quality, compactness and high stability [38-39]. Yb-doped fiber lasers have always been the research interest due to its merits such as high output and high slope efficiency. Since the invention of double-clad fiber, the output power of Yb fiber laser follows the Moore's law of fiber laser-Payne's law, i.e. the laser output doubles every two years. The 2μm laser wavelength from the Tm^{3+}-doped fiber laser is "eye-safe", which has wide applications in medical treatment, optoelectric Lidar and pump sources for mid-infrared lasers. Although Tm^{3+}-doped fiber lasers appear later than the Yb fiber laser [40], and the output power is lower than that of the latter, the output of the Tm^{3+}-doped fiber laser also follows Payne's law.

3.1.2 Limitation and advantages for power scalability of Tm^{3+}-doped fiber lasers

1. Energy levels of the Tm^{3+}-doped fiber laser

In Tm^{3+}-doped fiber lasers, the 2μm laser light comes from the transition $^3F_4 \rightarrow {}^3H_6$. the energy level diagram of Tm^{3+} ions is shown in Fig. 15 [41]. Due to strong Stark splitting of the $^3F_4$ level, the Tm^{3+}-doped laser is a quasi-four-level laser system. Besides, ions have a much smaller absorption cross section of 1.14×10^{-21}cm^2 [40] than that of Yb^{3+} ions (7.7×10^{-21}cm^2). Therefore, the Tm^{3+}-doped fiber laser requires more bright pump diode lasers to over its threshold. For the $^3F_4$ upper laser level, the emission cross section is $\sigma_{emi}=0.6\times10^{-21}$cm^2 [40]. The saturation intensity can be calculated from the expression [42]

$$I_{sat} = \frac{h\nu}{\sigma_{emi}\tau_f}, \tag{1}$$

where τ_f is the lifetime of the upper laser level.

From the calculation, we obtain the saturation intensity I_{sat} = 0.5kW/cm^2.However,the present output laser intensity of Tm^{3+}-doped fiber lasers has arrived at 2GW/cm^2, far over the saturation intensity. Therefore, high extraction efficiencies near quantum limitation can be achievable. In practice, the accessible laser efficiency is influenced by the physical-chemical features (spectrum, clustering, solubility and re-absorption, et al) of Tm^{3+} ions doped in silica fibers. The doping level of Tm^{3+} in silica fibers is usually lies in the 5000ppm level, and the fiber length is less than 13 meters. These conditions play a basic limitation in the output and energy-storing capability for the Tm^{3+}-doped silica fiber laser.

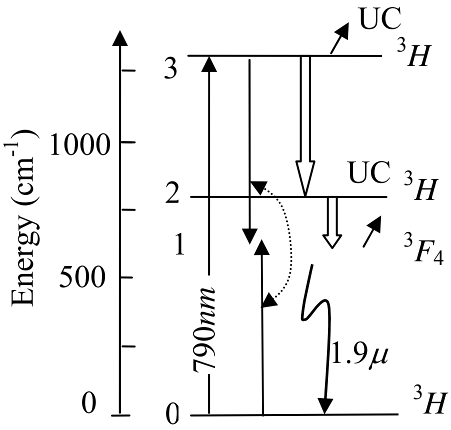

Fig. 15. Diagram of the energy levels of Tm^{3+} ions

2. Optical damage

Optical damage to fiber is always a factor should be considered when high power output is expected from fiber lasers, because the optical damage of fiber set a upper limit for achieved power. Optical damages to fiber mainly include the material damage by instant light intensity and the photo-darkening effect by long-time illumination. In order to obtain single-transverse-mode operation, the normalized frequency of fiber should be

$$V = \frac{\pi \cdot d \cdot (N.A.)}{\lambda} < 2.4 \tag{2}$$

Where, d is the fiber diameter, and N.A. is the fiber numerical aperture. Limited by the fiber drawing technique and bend loss, the N.A. of fiber is generally less than 0.06. Therefore, the diameter of single-mode fiber cannot be too large. To obtain the same V, 2μm-fiber can have a diameter twice that of 1μm-fiber, thus a cross section of 4 times larger. Therefore, the Tm^{3+}-doped fiber is more preferred to achieve single-mode high power laser output.

Damage to bulk fiber

The damage to silica fiber by high-power laser is a complicate process, including many factors such as local heating induced glass fracture, glass evaporation, and non-linear effects, et al. By using 1-μm laser in measurement, damage threshold of silica fiber was obtained from 16GW/cm^2 to 400GW/ cm^2, showing great discrepancy. When Yb^{3+} ions are doped, the damage threshold will decrease to be 0.5~0.8 times that of the pure silica fiber [43]. As far as the fiber facet is considered, the damage threshold will drop to 1/4 times that of pure silica fiber due to the impact of surface plasma, being about 40GW/cm^2 [44]. For the passive components in fiber lasers, such as fiber gratings, coated mirrors and fiber couplers, the damage threshold will be further decreased. At present, the maximum light intensity achieved in 1μm fiber laser is 2GW/cm^2, much lower than the fiber damage threshold.

As shown in Fig. 16, the silica fiber has much stronger absorption at 2μm wavelength than at 1μm wavelength. Therefore, the silica fiber damage threshold will be lower at 2μm wavelength (~40GW/cm^2) than at 1μm wavelength. On the other hand, the surface plasma effect will be smaller by 2μm laser, which will improve the damage threshold to some extent. In experiment, the 2μm laser light intensity achieved in the Tm^{3+} fiber has arrived at $2GW/cm^2$, being the same order of magnitude with that of 1μm laser.

As far as short-pulse (ps to ns regime) lasers are concerned, when neglecting self-focusing and other factors, the damage threshold of silica fiber follows the integrating law, which can also be applied to silica fiber laser [43].

$$E_{thres} \approx \sqrt{2/\pi} P \Delta t \ , \tag{3}$$

where, P is peak power and Δt is the pulse width. The damage threshold peak power P= $475GW/cm^2$ is nearly unchanged [43], indicating that heating effect is not the mail factor leading to fiber damage. For fs-level laser pulses, self-focusing will be the primary source of fiber laser, and eq. (3) cannot be used.

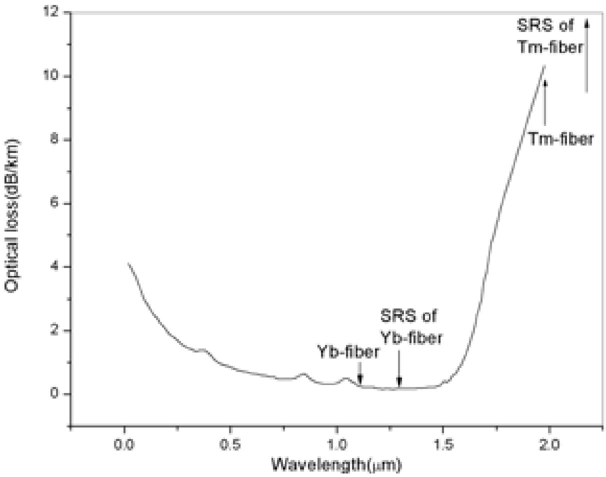

Fig. 16. Optical loss of Yb and Tm lasers, and their respective SRS emissions in silica fiber

Photo-darkening

Photo-darkening is the phenomenon that, after long time of laser operation, high-energy photons will induce color-center and defects in silica fiber, thus lead to growth of laser absorption and decrease of laser efficiency. Photo-darkening mainly stems from the radiation of UV and visible light. After 4 hours' radiation of 5 mW laser light at 488 nm, photo-darkening can be clearly observed. The photo-darkening-induced absorption primary occurs in the UV and visible spectral range. However, due to the fact that silica fiber itself has very weak absorption at the 1~2μm wavelength range, even slight photo-darkening will reduce the efficiency of fiber lasers [45].

Photo-darkening is extensively observed in Tm^{3+}-doped fiber lasers. Therefore, photo-darkening was considered a hamper limiting long-time operation of Tm^{3+}-doped fiber lasers pumped by 790 nm diode lasers. However, present experiment has shown that Tm^{3+}-doped fiber laser can operate stably over 2000 hours [46], close to that of Yb fiber lasers. Employing pre-radiation with UV light will decrease photo-darkening effect, thus enhance the lifetime of Tm^{3+}-doped fiber lasers.

3. Thermal issues

Larger ratio of surface to volume of fiber provides fiber lasers a good heat management system [47]. The heat generated in fiber core through multiphonon relaxation can be effectively dissipated by radiation and convection from the outer surface of the fiber. Most important is that, due to the guiding effect of fiber, even large temperature gradient exists will not deteriorate the light beam quality severely. However, with enhancement of output power, thermal issues of the Tm^{3+}-doped fiber laser become serious and should be considered carefully.

Heat effects

Just as the Yb fiber laser, the key factor deciding how high power the Tm^{3+}-doped fiber laser can endure is the melting temperature of the fiber core. By adopting positive cooling, the heat resistance ability of the Tm^{3+}-doped fiber laser is about 100 W/m.

The 790nm-pump Tm^{3+}-doped fiber laser has the "one-for-two" energy-transfer process-cross relaxation [23], there exist three transitions leading to occurrence upper laser level ions from absorbing a pump photon. They are (1) $n_3 \rightarrow 2 \cdot n_1$ (cross relaxation); (2) $n_3 \rightarrow n_2 \rightarrow n_1$; and (3) $n_3 \rightarrow n_1$. Taking into account the up-conversion and re-absorption, the quantum efficiency of achieving upper laser level ions is

$$\eta = [2\eta_{3101} + \eta'_{3101} + \eta_{3201}]\eta_{las} - \eta_{up} - \eta_{reabs} \tag{3}$$

Neglecting some weak effects, the expression can be simplified to

$$\eta = 2\eta_{31} + (1 - \eta_{31})(\beta_{31} + \beta_{32}) \tag{4}$$

From the parameters of Tm^{3+}-doped silica fiber, we can obtain $\eta = 0.74$, which is comparable with that of Nd:YAG laser. The quantum efficiency of Tm^{3+}-doped fiber laser is also related to the doping concentration, operation temperature and other cavity parameters. Based on the heat management capability, it is concluded that the Tm^{3+}-doped fiber laser can provide a output potential of about 300W/m.

Efficiency decrease by operation temperature

The ground state energy level of Tm^{3+} ions is consisted of a series of sublevels, forming a continuous energy band with a broad bandwidth of 5770 cm^{-1} [48]. This feature provides the Tm^{3+}-doped fiber laser a quasi-four level laser system, possessing high temperature stability. At kilowatt level, the reduction of population inversion of Tm^{3+}-doped fiber laser due to temperature growth is less than 1%.

Based on a 5.5cm-length Tm^{3+}-doped fiber laser, the influence of temperature on the laser's efficiency has been observed, as shown in Fig. 12. When the temperature is increased from 10°C to 40°C, the output and slope efficiency decrease about 30% [33]. The primary reason leading to the reduction of output power is the 0.3nm/°C wavelength shift of the pump diode laser, which making the pump light cannot overlap well with the Tm^{3+} absorption band, decreasing the pump absorption efficiency. If only the absorbed pump power is taken into account, the power reduction is just 5%. Another alternative explanation is that the fluorescence spectrum of Tm^{3+}-doped fiber is broadened with temperature, decreasing the gain per unit-length of fiber. As far as long fiber lasers are concerned, the influence of these